Al-Qadisiyah Journal of Pure Science

Volume 25 | Number 3 Article 14

7-7-2020

The Structural, Magnetic, And Optical Properties Of Cu1-xCoxFe2O4 Spinel Ferrite And Its Applications

Saleem Hamza Trier
Department of Environment, College of Science, University of Al-Qadisiyah, Diwaniyah, Iraq,,
Salem.altawel@qu.edu.iq

Mohammed Sami Abdali
Department of Environment, College of Science, University of Al-Qadisiyah, Babelon, Iraq,
mohammed.sami68@yahoo.com

Recommended Citation

Trier, Saleem Hamza and Abdali, Mohammed Sami (2020) "The Structural, Magnetic, And Optical Properties Of Cu1-xCoxFe2O4 Spinel Ferrite And Its Applications," *Al-Qadisiyah Journal of Pure Science*: Vol. 25: No. 3, Article 14.
DOI: 10.29350/qjps.2020.25.3.1122
Available at: https://qjps.researchcommons.org/home/vol25/iss3/14

Al-Qadisiyah Journal of Pure Science
ISSN(Printed): 1997-2490 ISSN(Online): 2411-3514
DOI: /10.29350/jops.
http://qu.edu.iq/journalsc/index.php/JOPS

The structural, magnetic, and optical properties of $Cu_{1-x}Co_xFe_2O_4$ spinel ferrite and its applications

Authors Names
a. Saleem Hamza Trier

b. Mohammed Sami Abdali

Article History
Received on: 20/4/2020
Revised on: 10/5/2020
Accepted on: 16/5/2020
Keywords:
Spinel ferrite, PLD, Sol-gel, $CuFe_2O_4$, Magnetic properties, glass substrate.

DOI: https://doi.org/10.29350/jops.2020.25. 3.1122

ABSTRACT

In this paper, the nanoparticles of the spinel ferrite ($Cu_{1-x}Co_xFe_2O_4$) were prepared using the sol-gel method at a calcined temperature of 600 °C for 6 hours at the cobalt content (x=0,0.3,and 0.5). The XRD analysis of the nanoparticles confirmed the formation of a tetragonal spinel structure free of unwanted phases, single-phase and transform into a cubic spinel structure when cobalt content ratio (x=0.5). The crystalline size and lattice constants increase with increasing cobalt content there was a significant increase in the density of x-rays when the crystal structure turned into a cubic system. SEM images showed that spherical nanoparticles of pure copper ferrite films were distributed of regularly over a substrate of glass their crystalline size (62.25-60.0) nm, and their crystalline size decreased to (31.25-33.33) nm ,and their accumulation increases when proportion of cobalt content(x=0.5). EDX established that nanosamples contained the elements Fe, Mg, Co, and O, and that there were no additional elements, and when the proportion of cobalt content increased (x=0.5), the iron ions decreased at the tetrahedral site A. The magnetic properties of the copper ferrite powder were studied using the (VSM), and it was noted that the tetragonal system shifted to a cubic system when the ratio of the cobalt content (x=0.5). The significant increase in magnetic parameters (Ms, Mr and n_B (μ_B)) and the tightness of the hysteresis loop make it a soft magnetic material, so it can be used in high frequency magnetic equipment. The properties of optical the membranes prepared by UV-Is spectroscopy were studied and showed high transmittance at the percentage of cobalt content (x=0.5) between (80-90)% in the visible and infrared region. At the ratio (x=0.5) the energy gap and the dielectric constant increase, making it useful for devices photodetector and gas sensors.

MSC:

[a] Department of Environment, College of Science, University of Al- Qadisiyah, Diwaniyah, Iraq, E-Mail: Salem.altawel@qu.edu.iq or 1967saleemhamza@gmail.com
[b] Department of Environment, College of Science, University of Al- Qadisiyah, Babelon, Iraq, E-Mail: mohammed.sami68@yahoo.com

1. Introduction

The formula AB_2O_4 indicates to spinel ferrite, which are a very large class of oxides that is applied in a very wide range in the industry starting from simple permanent magnets to microwave, magnetic recording, gas sensors[9], photo catalysts, water treatment catalysts, and air purification systems [14,15]. To preparation ferrite films [8], there are many methods to prepare ferrite films such as sol-gel method ,plating of ferrite, the chemical method[11], electro deposition method, sputtering, RF sputtering and spray pyrolysis[3]. The considered the nanostructure of ferrite films is an important parameter in determining magnetic properties[13]. There are many factors that affect the nanostructure of ferrite films, such as the substrate temperature [10], coefficient of thermal expansion and lattice mismatch between substrate and target [1]. Copper ferrite $Cu_{1-x}Co_xFe_2O_4$ is one of a reverse spinel ferrite and has important basic properties such as thermal and chemical stability[21]. And it is a unique material that offers low-loss performance at high frequencies due to their high electrical resistance, high permeability and their high magnetization salts for oxide materials. In the spinel structure, oxygen ions constructs a close packed lattice with cations and distributed in tetrahedral A and octahedral B sites in transitional mineral materials (d), and that magnetic and electronic properties are responsible for determining the balance and distribution of these cations. Ferrite of the copper ($Cu_{1-x}Co_xFe_2O_4$) is partially inverted spinel in which 85% of Cu^{2+} cations occupy sites B and 15% at A site [18], and it often can be written according to the formula$(Cu^{2+}{}_{1-x}Fe^{3+}{}_x)_A$ $[Cu^{2+}{}_xFe^{3+}{}_{2-x}]_BO_4$, where that brackets of circular and square indicate the locations of tetrahedral cations(A) and octahedral (B), and x denotes the ratio of the content of matter additives occupied by the cations, where that ferrite cobalt is a natural spinel occupies the A site [25,22,26,7]. This work aims to prepare copper ferrite nanoparticles by using the sol-gel method, to see the result of adding cobalt content proportions, study their physical properties and determine their application fields.

2. Experiments

$Cu_{1-x}Co_xFe_2O_4$ (copper ferrite) was prepared with certain proportions of cobalt content (x=0, 0.3 and 0.5) using a sol-gel method to synthesize copper and cobalt ferrite. In this process, high purity metal nitrate was used to avoid the effects on the properties of spinel ferrite. The process was carried out in two stages in the first stage, copper nitrate, ferric nitrate and citric acid were mixed in equal ratios, and dissolved in 100 mol of distilled water in a heat-resistant glass cup to obtain a pure copper ferrite. In the second stage, copper nitrate, ferric nitrate, citric acid and cobalt nitrate were mixed in the above-mentioned proportions, both separately, and the molecular weight of the pure and mixed materials was calculated as in table 1. Magnetic stirrer was used to obtain a homogeneous

solution after the mixed materials are completely dissolved. Then added the ammonia

solution to the homogeneous solution to raise the pH to (~7). The temperature of the hot magnetic stirrer was gradually increased until the gel becomes dry ,and then the temperature was increased further until the dry gel was completely burned in the spontaneous combustion process and turned into burning ash. This process is carried out in the first and second stages. Burnt ash was collected and crushed by an electric mill for 10 min. to obtain ferrite powder of fine copper. It was calcined at 600°C for 6 h. and then crushed again. The powder was examined using XRD technique to determine the composition of the spinel structure, and also examined using a vibrating sample magnetometer (VSM) to determine its magnetic properties. The powder was mixed with 6% by weight of matter glycerin as a binder. The powder was pressed using an electrostatic piston (40 kN) to obtain circular samples weighing (5g) with diameter (3cm) according to the proportions mentioned above in the copper- cobalt ferrite. The samples were calcined at 1000 °C for 6 h. The glass substrates were used with dimensions (4.6×2.5×0.1) cm^3 and they were cleaned by two stages. In the first stage, ethanol was used to remove dust and fats that may be present on its surface. In the second stage, they were submerged in distilled water for a period of (15 minutes) using the ultrasound machine then they were dried in a thermal oven for 15 minutes. The thin films of copper ferrite were prepared in the above ratios by using a pulse laser deposition (PLD) technique in a high-vacuum chamber(10^{-3}mbar), by mechanical pump. Then the glass substrates were fixed inside the deposition system and the distance between the substrate and the sample was (5cm). The Nd: YAG type laser beam with 1064 nm wavelength was used to study the optical and morphological properties of the copper ferrite prepared films.

Weights of raw materials used in the research were calculated from their molecular weights as below:

$Fe(NO_3)_3.9H_2O = (1 \times 55.850) + (3 \times 14.01) + (18 \times 16) + (18 \times 1.008) = 404.024$ g/mol

$Co(NO_3)_2.6H_2O = (1 \times 58.930) + (2 \times 14.01) + (12 \times 16) + (12 \times 1.008) = 291.046$ g/mol

$Cu(NO_3)_2.6H_2O = (1 \times 63.546) + (2 \times 14.01) + (12 \times 16) + (12 \times 1.008) = 295.662$ g/mol

$C_6H_8O_7.H_2O = (6 \times 12.010) + (10 \times 1.008) + (8 \times 16) = 210.140$ g/mol

Calculated the molecular weights of copper ferrite ($Cu_{1-x}Co_xFe_2O_4$) by distributing cations on tetrahedral sites A and octahedral B according to the ratios of the added cobalt (x = 0.0, 0.3 and 0.5), as below:

$(Cu_{0.15}Fe_{0.85})_A[Cu_{0.85}Fe_{1.15}]_BO_4=(0.15\times63.546+0.85\times55.85)_A+[0.85\times63.546+1.15\times55.85]_B+(4\times 16) = 239.246$g/mol

$(Cu_{0.105}Co_{0.3}Fe_{0.595})_A[Cu_{0.595}Fe_{1.405}]_BO_4=(0.105\times63.546+0.3\times58.93+0.595\times55.85)_A+[0.595\times63.546+1.405\times55.85]_B+ (4\times16) = 237.861$ g/mol

$(Cu_{0.075}Co_{0.5}Fe_{0.425})_A[Cu_{0.425}Fe_{1.575}]_BO_4=(0.075\times63.546+0.5\times58.93+0.425\times55.85)_A+[0.425\times63.546+1.575\times55.85]_B+ (4\times16) = 236.938$ g/mol

Table (1): Calculating the molecular weights of copper ferrite $Cu_{1-x}Co_xFe_2O_4$ according to ratios of the cobalt content

Cobalt content(x)	Copper ferrite	$Fe(NO_3)_3$ $.9H_2O$	$Cu(NO_3)_2$ $.6H_2O$	$Co(NO_3)_2$ $.6H_2O$	$C_6H_8O_7$ $.H_2O$	$2Fe(NO_3)_3$ $.9H_2O$	$2C_6H_8O_7$ $.H_2O$	Cu_{1-x} $Co_xFe_2O_4$
0.0	$CuFe_2O_4$	404.023	295.661	291.045	210.139	808.047	420.27	239.246
0.3	$Cu_{0.7}Co_{0.3}Fe_2O_4$	404.023	295.661	291.045	210.139	808.047	420.27	237.861
0.5	$Cu_{0.5}Co_{0.5}Fe_2O_4$	404.023	295.661	291.045	210.139	808.047	420.27	236.938

3. Results and Discussion

3.1. Structure Properties

Figure1 illustrates x-ray powder diffraction patterns for ($Cu_{1-x}Co_xFe_2O_4$) nanoparticles prepared by using the sol-gel method with cobalt content ratios (x=0, 0.3 and 0.5). XRD showed typical peaks of the crystalline levels (101), (112), (103), (211), (202), (220), (321), (224) and (400) which correspond exactly to the standard cards JCPDS (6-545) and (25- 283). XRD confirmed the formation of a single-phase tetragonal spinel ferrite with a polycrystalline nature and no phase of impurities appeared in the ferrite samples. It is turn into ferrite spinel cubic when the cobalt content ratio(x=0.5), but the prevailing direction does not change.

In $Cu_{1-x}Co_xFe_2O_4$ structure, cations occupy 85% in octahedral sites (B) whereas be, 15% in tetrahedral sites (A) [18].When the cobalt content ratios increase, the crystalline size is increases, and the lattice parameters increases too. At the ratio x=0.5 the structure of spinel ferrite is turns into a cubic shape (a=b) and the best distribution of the cations is occurs i.e., the crystallization is improves and the crystalline defects decrease. The crystalline size D_S of the copper ferrite is calculated for plane (211) according to equation (1) which is Debye Scherer formula [17]:

$$D_S = \frac{k\,\lambda}{\beta\,\mathrm{Cos}\,\theta} \qquad (1)$$

Where k is constant, λ is the x-ray wavelength, β is the full width at half the maximum, measured in units (radians), θ is angle of Bragg. The crystalline sizes have been shown to increase with increasing cobalt content ratios (30.357, 45.256 and 49.637) nm, as shown in table 2. This depends on the basis that copper based spinel nanoparticles are more be accurate with the substitution of cobalt ions. In a certain ratios of copper-cobalt ferrite,

cations of copper ions can occupy tetrahedral and octahedral sites (A and B), but in

certain ratios. Whereas cobalt ions occupy only the tetrahedron sites A. The increase in the cobalt content ratios leads to an increase in the lattice parameters (a and c) as shown

in table 2. This increase can be attributed to that the Co^{2+} ion radius greater than the Cu^{2+} ion radius, at the ratio (x=0.5) the crystalline system turns from the tetragonal system to the cubic system, and calculated from the equations (2 and 3) [17,12]:

$$\frac{1}{d_{hkl}^2} = \frac{h^2+k^2}{a^2} + \frac{l^2}{c^2} \qquad (2)$$

$$d_{hkl}^2 = \frac{a^2}{h^2+k^2+l^2} \qquad (3)$$

Where h, k and l are the coefficients of Miller for crystalline levels. The addition of cobalt ions reduces macro strain (S) in copper ferrite samples, because the cobalt ion radius is greater than the copper ion radius. The macro strain value can be calculated from equation (4) [9].

$$S = \frac{\beta \cos\theta}{4} \qquad (4)$$

The density of the dislocation (δ_D) is inversely proportional to the square of crystallite size and is depend on it. The density of dislocation increases as a result of defect occurrence in an entire row within the crystalline structure and is considered from the crystalline defects, and its calculated from the equation (5) [9]:

$$\delta_D = \frac{1}{D_s^2} \qquad (5)$$

The density of x-ray in the cubic system for the copper-cobalt ferrite increases, and decreases in the tetragonal system due to the decrease in the cell unit volume in the cubic system with increase the ratios of cobalt content as in table 2, and the density x-ray was calculated from the equation (6) [20].

$$P_x = \frac{4M}{NV} \qquad (6)$$

Where M the molecular weight of ferrite, N the number of Avogadro and its amount (6.023×10^{23} mol^{-1}) and $V= a^2c$ the volume of cell unit and component from 4 units.

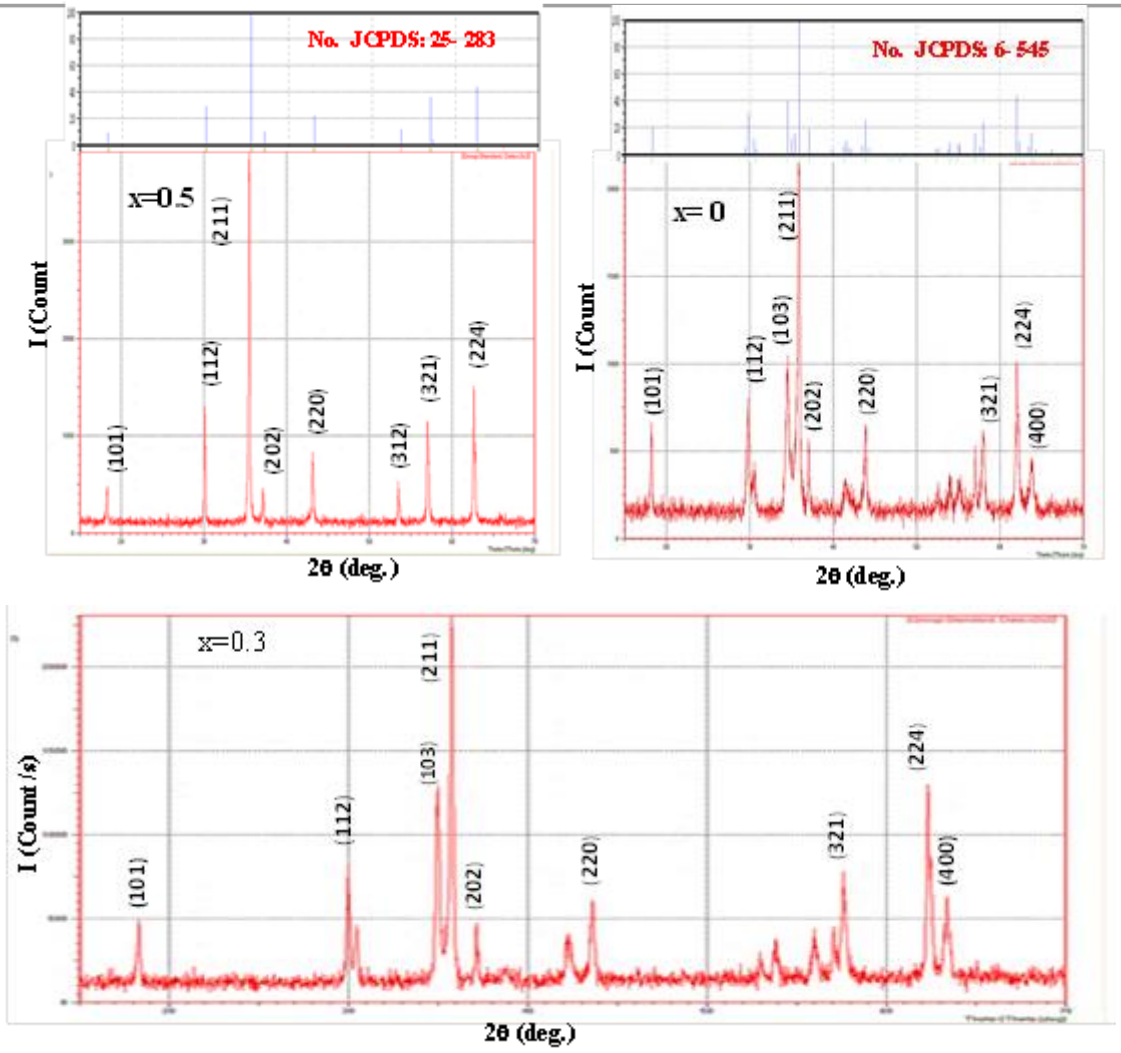

Figure 1: X-ray diffraction patterns (XRD) for $Cu_{1-x}Co_xFe_2O_4$ copper powder ferrite for the cobalt content ratios (x=0, 0.3, and 0.5) with the standard cards for each ratio

Table (2): Shows the constants of lattice (a) and (c) , volume of unit cell (V), density of x-ray (P_x), the crystalline size (D_s), density of dislocation (δ_D) and macro strain (S) of copper ferrite $Cu_{1-x}Co_xFe_2O_4$ when ratios of cobalt content (x = 0,0.3, and 0.5)

Cobalt content (x)	lattice constants a(Å)	c(Å)	V(Å)^3	P_x (g cm^{-3})	D_s (nm)	$\delta_D \times 10^{14}$ (lin m^{-2})	$S \times 10^{-2}$ (lin^{-2} m^{-4})
0.0	5.837	8.620 (Tetragonal)	293.688	0.541	30.357	10.85	6.540
0.3	5.856	8.647 (Tetragonal)	296.529	0.533	45.256	4.880	4.387
0.5	6.192	6.192 (Cubic)	237.410	0.663	49.637	4.060	4.000

3.2. Morphology of Surface

The morphology form and size granular of nanoparticles can be projected of SEM images. Figure 2 (A and B) shows the morphology of ferrite films (copper and cobalt) $Cu_{1-x}Co_xFe_2O_4$ for the cobalt ratio (x=0 and 0.5). Figure2a shows a homogeneous dense surface and forms a spherical morphology of a granular size of (60.0-62.5) nm. The small conglomerates form into large particles free from cracks and voids, the conglomerates is due to the magnetic nature of the cobalt ions. At the cobalt ratio (x=0.5) the conglomerates of the nanoparticles increases, and is due to the increase in the magnetic moment of the Co^{2+} ions and the granular size decreases from (31.25-33.33) nm as shown in figure(2B). The EDX energy analysis allows to determine of compound components and their percentages. Figure2(a and b) show EDX spectrum for the copper ferrite $Cu_{1-x}Co_xFe_2O_4$ to verify samples. The peaks distinctive of spectrum contain elements Co, Cu, Fe and O. The EDX confirmed the homogeneous mixing of Co, Cu and Fe elements and the purity of the chemical compound. The percentage of Fe^{2+}ion was shown to decrease in a tetrahedral A site by increasing the cobalt ratio as in the table involved with figure 2b. The attached two tables with the two figures shows the quantitative estimation of the directly obtained elements of the spectrum by their ratios and weights atomic.

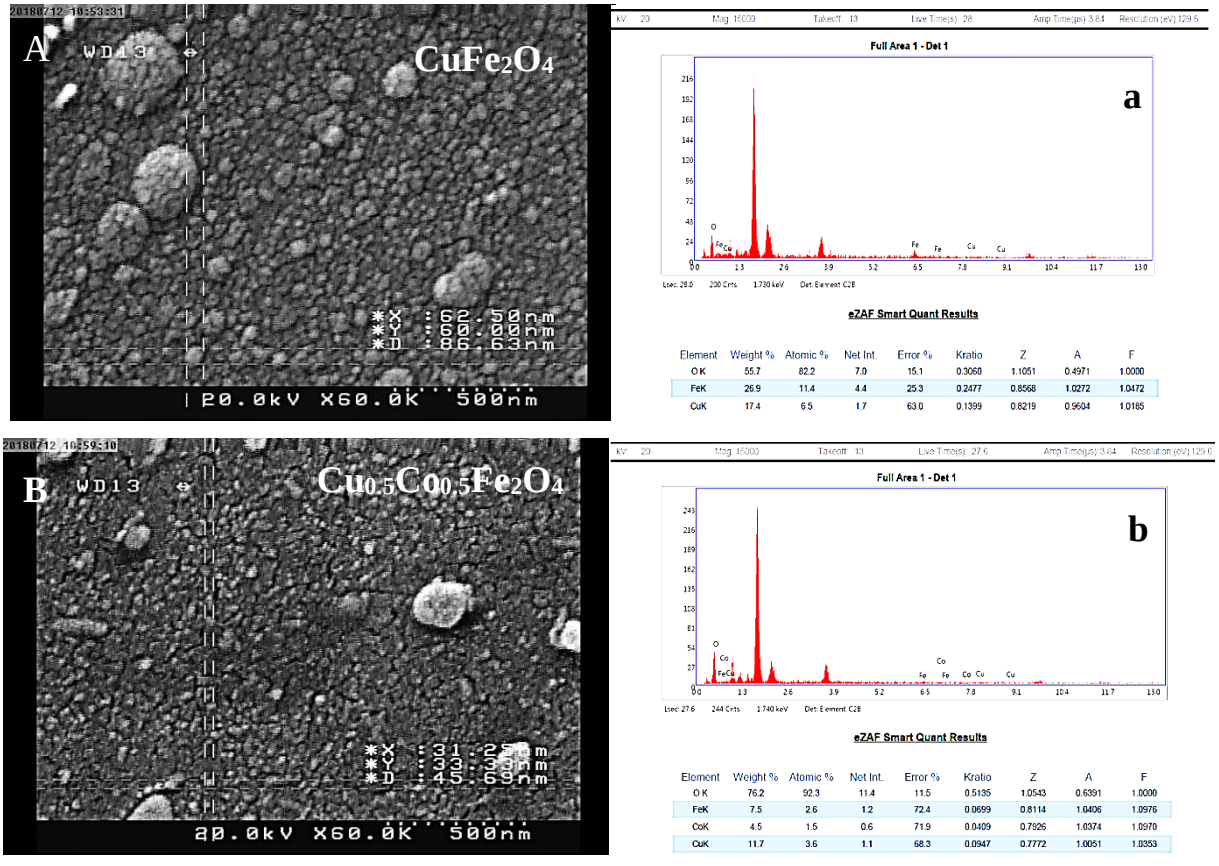

Figure 2(A,B): Illustrates SEM images of $CuFe_2O_4$ and $Cu_{0.5}Co_{0.5}Fe_2O_4$ ferrite with their EDX spectra and their accompanying tables.

4. The Magnetic Properties

The magnetic properties of copper ferrite samples were studied using the (VSM) when apply an external magnetic field at room temperature. The results showed that all samples were saturated of magnetic as in figure4. That all the magnetic parameters such as saturation of magnetization (Ms), the remnant of magnetic (Mr), coercivity (Hc), ratio of squareness (Mr/Ms) and constant of anisotropy (K_1), were their obtained of the magnetic hysteresis loop for prepared samples.The magnetic moment value of samples the prepared can be determined from equation (7) [20].

$$n_B\,(\mu_B) = \frac{M_w \times M_s}{5585} \qquad (7)$$

We would like to highlight an important case, that the reactions (A-A), (B-B) and (A-B) are the reactions of the basic magnetic that occur in spinel ferrite, and the interaction of the last magnetic was the strongest. Increasing of magnetization saturation (M_s), magnetic (M_r) and magnetic moment $n_B(\mu_B)$ are observed when the ratio of cobalt in the copper ferrite increased as shown in table 3. This is due to the mutual effect of cations Fe^{3+} in site an octahedral B and Co^{2+}cations in tetrahedral A site, both of which are in increasing state as in equations for calculating the distribution of cations .The highest value has found of the squareness ratio M_s/M_r when was the cobalt ratio (x=0.3) and decrease with increasing cobalt content, and this is due to the variable direction of magnetic remnant is incompatible with direction of magnetization saturation. The spinel ferrite shown high magnetization saturation and high magnetic moment with a narrow magnetic hysteresis loop when cobalt ratio (x=0.5) as shown in figure3 and table 3, and this is the behavior of the soft magnetic materials. It was observed the highest value for the anisotropic constant (k_1) when cobalt ratio (x=0.3) this due to increase in coercivity (H_c), and its value can be determined according to equation (8) [20, 19].

$$k_1 = \frac{M_s \times H_c}{0.96} \qquad (8)$$

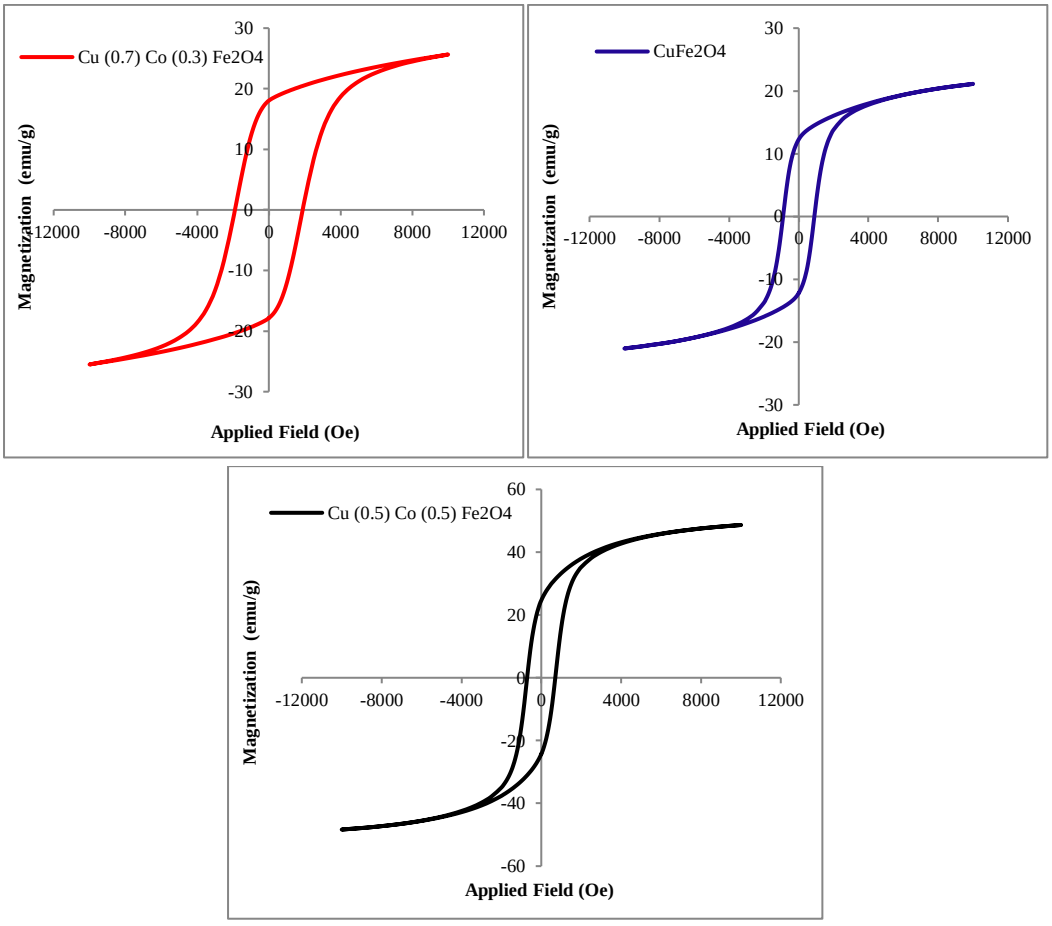

Fig. 3: The magnetic hysteresis loops of copper ferrite $Cu_{1-x}Co_xFe_2O_4$, in cobalt content ratios
(x = 0, 0.3 and 0.5)

Table 3: Shows the magnetic parameters of copper ferrite $Cu_{1-x}Co_xFe_2O_4$, in cobalt content ratios (x = 0.0, 0.3,and 0.5)

Cobalt content (x)	Ms (emu/g)	Mr (emu/g)	Hc (Oe)	Mr/Ms	$K_1\times10^4$(erg/g)	$n_B(\mu_B)$
$CuFe_2O_4$	21.12	12.28	900	0.581	1.980	0.905
$Cu_{0.7}Co_{0.3}Fe_2O_4$	25.65	18.03	1900	0.703	5.077	1.092
$Cu_{0.5}Co_{0.5}Fe_2O_4$	48.66	24.64	700	0.506	3.548	2.064

5. Optical Properties

The consider optical properties are very important and play a major role in the semiconducting thin films of transparent oxides through which the fields of application of these films can be determined. Figure4 shows the optical absorbance spectra, optical transmittance and some optical properties of $Cu_{1-x}Co_xFe_2O_4$ thin films of the cobalt content ratio (x=0 and 0.5) as a function of the wavelength in the spectral range (300-900) nm. All optical parameters increase when the cobalt content increases, and the optical transmittance ranges from (80-90)% in region of the visible and infrared rays as in Figure 4B, which makes these films good for solar cell applications. These results are consistent with the researcher [6]. Pure copper ferrite films can be used as UV protective films for electronic and optical devices because these films have less than 35% transmittance in the UV region. Thin-film reflectivity depends on the absorbance spectrum and optical transmittance, and Figure 4C shows the reflectivity spectrum as a function of the wavelength. The absorption coefficient (α) can be calculated according to equation (9) [23] based on absorbance spectrum of the copper ferrite membranes. Figure 4D shows the change in the coefficient of absorption (α) as a function of wavelength, and was noticed that reduce with increasing wavelength due to increased crystallization of membranes, which in turn decreases crystalline defects, as well as decrease localized levels within the energy gap caused by the defects in the crystalline structure.

$$\alpha = 2.303\frac{A}{t} \qquad (9)$$

Where that A the absorbance, t thickness of the membrane. The absorbed ray in matter reacted, which leads to electronic transitions between the valence package and the conduction band is into direct and indirect transitions and these transitions were described by the Tauc equation , equation (10) [9,2]:

Where (hν) is energy of photon, (n) constant and takes the values (1/2 and 2/3) according to the matter and the type of the optical transmittance , either direct or indirect, and B is constant. The gap of energy was calculated from the relationship between $(\alpha h\upsilon)^2$ and hυ, and straightening the straight line which intersect with the x-axis at $(\alpha h\upsilon)^2=0$, as in figure 4E. It was observed that the gap of energy increases with increasing cobalt content from (3.41-3.62) eV.

Optical conductivity σ_{opt} can be calculated from equation (10) and it has been observed that it increases at an increase the ratio of cobalt content, and this is due to the increase in the extinction coefficient because it depends on it as in the figure 4F.

$$(10)\sigma_{opt} = \frac{\alpha nc}{4\pi}$$

From the equation (11) was calculated refractive index, its value was increasing due to the increase in the cobalt content, because increase in the extinction coefficient and the reflexivity, both of which are in increasing state as in figure 4G.

$$n = \sqrt{\left(\frac{4R}{(R-1)^2} - k^2\right)} - \frac{(R+1)}{(R-1)} \qquad (11)$$

Where n is the refractive index, R reflexivity , from the equation (12) was calculated extinction coefficient. The k is defined as the attenuation the electromagnetic wave inside the membrane. The extinction coefficient increases at the cobalt ratio (x=0.5) as in fig. 4K, indicating that these membranes are opaque [16,9]. It was observed that the attenuation increases with increasing cobalt ratio.

$$k = \frac{\alpha\lambda}{4\pi} \qquad (12)$$

The real (ε_r) and imaginary (ε_i) part for the dielectric constant was calculated of the two equations (13 and 14) [9]. It was noted that the part of real (ε_r) is greater because its related to the speed of light, and the part of imaginary (ε_i) is smaller because it is related to the energy of absorption. The two figures 4(L and M) illustrate the real (ε_r) and imaginary (ε_i) part for the constant of dielectric.

$$\varepsilon_r = n^2 - k^2 \qquad (13)$$

$$\varepsilon_i = 2n\,k \qquad (14)$$

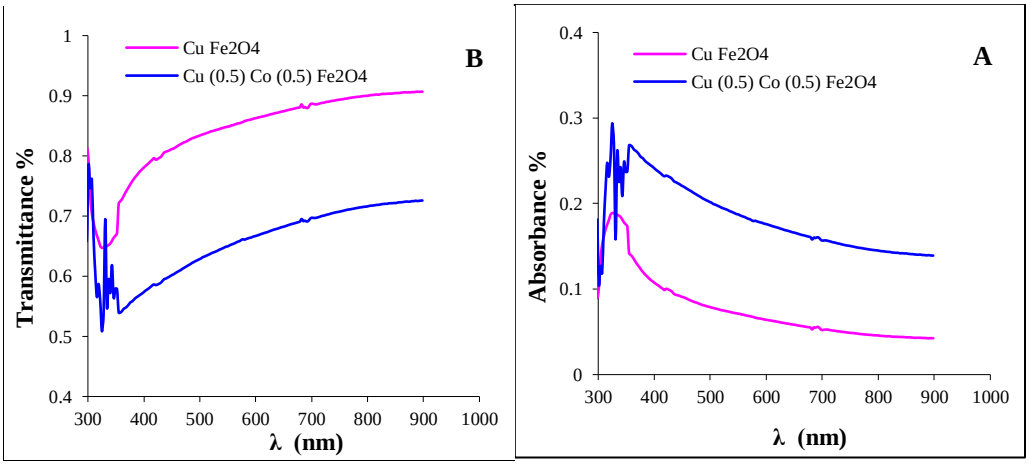

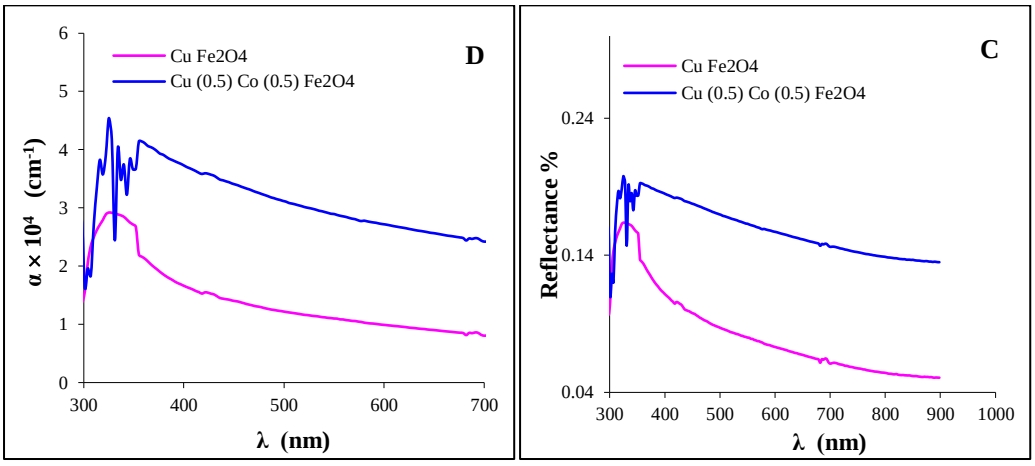
D
Cu Fe2O4
Cu (0.5) Co (0.5) Fe2O4
α × 10⁴ (cm⁻¹)
λ (nm)
C
Cu Fe2O4
Cu (0.5) Co (0.5) Fe2O4
Reflectance %
λ (nm)

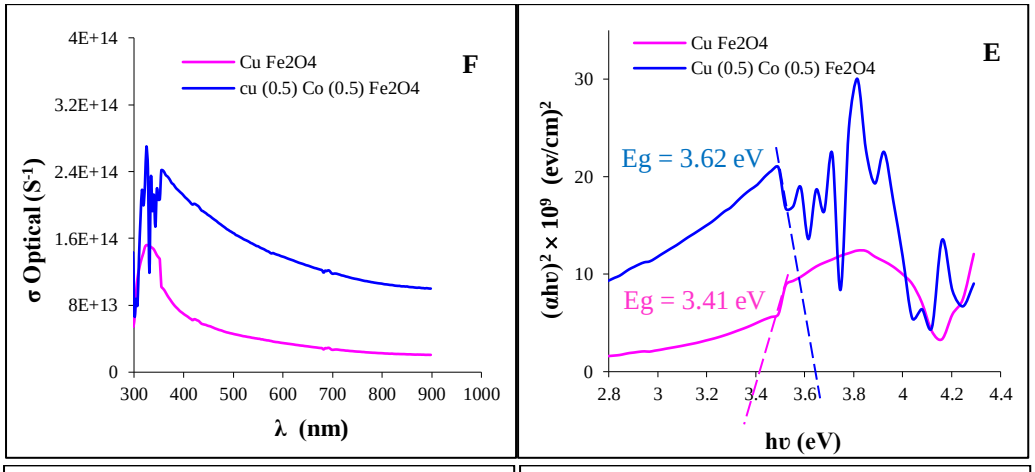
F
Cu Fe2O4
cu (0.5) Co (0.5) Fe2O4
σ Optical (S⁻¹)
λ (nm)
E
Cu Fe2O4
Cu (0.5) Co (0.5) Fe2O4
Eg = 3.62 eV
Eg = 3.41 eV
(αhυ)² × 10⁹ (ev/cm)²
hυ (eV)

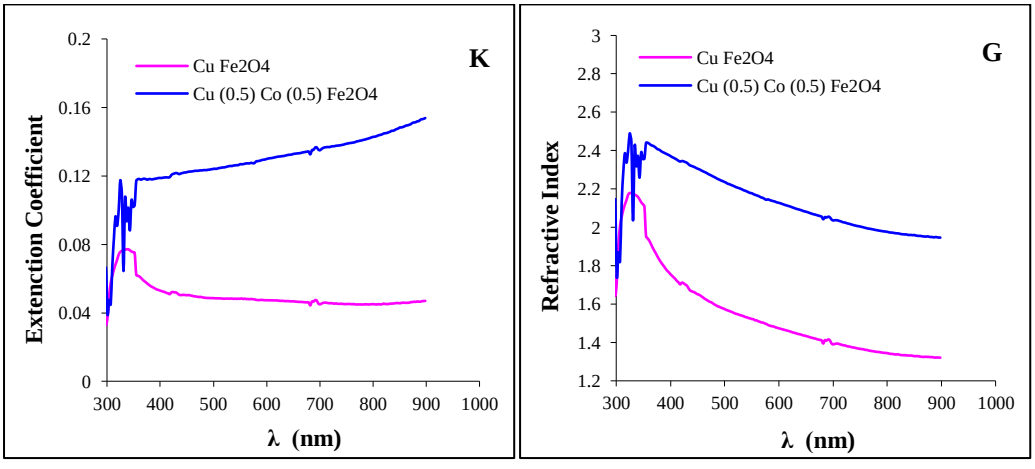
K
Cu Fe2O4
Cu (0.5) Co (0.5) Fe2O4
Extenction Coefficient
λ (nm)
G
Cu Fe2O4
Cu (0.5) Co (0.5) Fe2O4
Refractive Index
λ (nm)

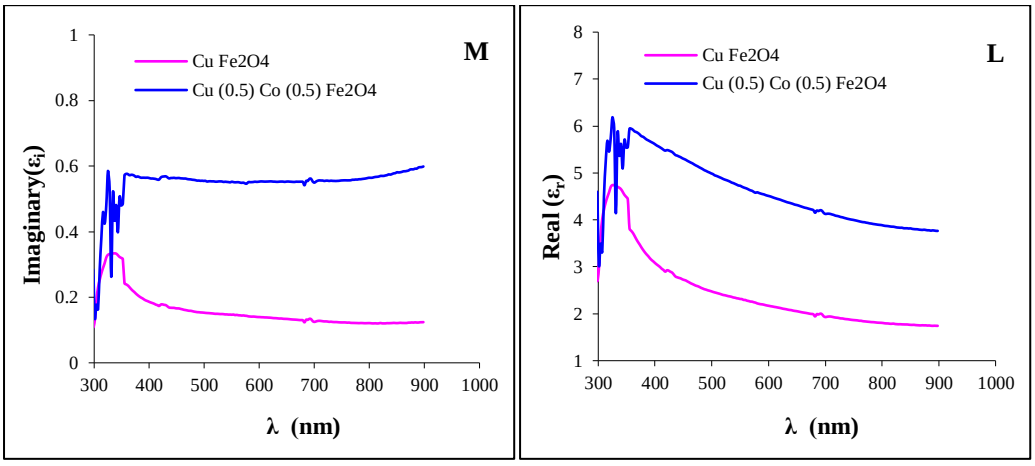

Figure 4(A, B, C , D, E, F,G, H, K, L, and M): The optical properties spectra of copper ferrite membranes $Cu_{1-x}Co_xFe_2O_4$, in cobalt proportion (x=0, and 0.5)

6. Conclusions

Copper ferrite was synthesized at ratios (x=0, 0.3 and 0.5) by using the sol-gel method. It was found that samples were crystallized in formation a tetragonal spinel of single-phase free from all unwanted phases and turns into a single-phase cube when the cobalt proportion (x=0.5). That the cations Fe^{2+} were found to decrease in tetrahedral A sites and it increase in octahedral B sites when ratio of cobalt content (x=0.5). This indicates that Cu^{2+}ions were distributed in both the octahedral and tetrahedral sites, whereas Co^{2+}ions in the (A) site. That the constants of lattice were found to increase when ratio of cobalt content (x=0.5), while the x-ray density decrease. The grain size decreases in the form of surface morphology and distribution of Fe^{2+} cations increase in octahedral B sites when the cobalt content increased. Thus the mutual effect increases and the magnetic moment increases, this is the base reason that leads to the increase in the magnetization of saturation. Ultraviolet spectroscopy confirms an increase in the optical energy gap, optical conductivity and transmittance for thin films when a cobalt content ratio (x=0.5).

This is due to an increase in crystalline size and a decrease in the crystal defects represented by the density of dislocation and macrostrain. The XRD technique confirmed the formation of a single-phase cubic spinel ferrite at the content ratio of the cobalt (x=0.5) and it is strongly affected by the addition of cobalt ions. The SEM images clearly showed the increase in the agglomeration in same ratio mentioned and decrease in the size of the spherical granules.

This is due to two reasons: the first is the increase in moment of magnetic in the sample and the second is the mutual effect between the sites (A) and [B] caused by the

increase in the distribution of Fe^{3+} cations in B site with the increase in the distribution of Co^{2+} cations in site A.

7. Acknowledgments

I would like to express my thanks and appreciation to Dr. Khadija Abees, Director of the Environmental Research and Pollution Prevention Unit and Mrs. Teaif, in the College Science of Al-Qadisiyah University for their continuous efforts to help me and allow me to work in their laboratories.

References

[1]. A. Manikandan, J. Judith Vijaya ,L. John Kenned and M. Bonoudina, "Structural ,optical and magnetic properties of $Zn_{1-x}Cu_xFe_2O_4$ nanoparticales prepared by microwave combustion method", Journal of molecular structure , 1035, (2013) , 338- 340.

[2]. A. Meenak shisundaram, N. Gunasekaran, and V. Srinivasan, "Distribution of metal ions in transition metal manganites AMn_2O_4 (A: Co, Ni, Cu, or Zn)". Physica Status Solidi(a), 69, (1982), 15-19.

[3]. A. Sankara Mahalingam, J.B. Lawrence, C.O. Augustin, Tenth National Convention of Electrochemists (NCE-10), Karaikudi, India, 26–27, (2001), p. 18

[4]. A. T. Raghavender, N. H. Hong, E. Chikoidze, Y. Dumont and M. Kurisu, "Effect of zinc doping on the structural and magnetic properties of nickel ferrite thin films fabricated pulsed laser deposition technique", Journal of Magnetism and Magnetic Materials, 378, (2015), 358-361.

[5]. Aria Yang, X. Zuo, L. Chen, Z. Chen, C. Vittoria, and V. G. Harris, "Magnetic and structural properties of pulsed laser deposited $CuFe_2O_4$ films" , Journal of Applied Physics 97, 10 , No. 107 , (2005) ,1-3.

[6]. B. Amraei, Rezaei Kalantary, R. Jonidi Jafari, A. M. Gholami, "Efficiency of CuFe2O4 bimetallic in removing amoxicillin from aqueous solutions" J. Mazandaran Univ. Med. Sci. 27, (2017), 259-275.

[7]. B.P. Ladgaonkar and A.S. Vaingankar, "In x-ray spectroscopy and allied areas", S.K. Joshi, B.D. Shrivastava, A.P. Deshpande (Eds.), Narosa: New Delhi, (1998) , p. 107 .

[8]. D. Anceila, G. Francisco Nirmala, P. Sagayaraj and V. Joseph , "Study on optical, magnetic and structural properties of $CuFe_2O_4$ by Co-precipitation technique", International Research Journal of Engineering and Technology, 4 Issue 9, (2017), 370–372.

[9]. D. K. Pawara, S. M. Pawarb, P. S. Patil and S. S. Kolekara,"Synthesis of nanocrystalline nickel–zinc ferrite ($Ni_{0.8}Zn_{0.2}Fe_2O_4$) thin films by chemical bath deposition method", Journal of Alloys and Compounds, 509, (2011), 3587-3591.

[10]. J. Gh. Alyasary, H. H . Almarmade and D. h. Altiee , "Study of structural and optical properties of the ferrite films prepared by chemical pyrolysis spray technique", Journal of Physics: Conf. Series 1032, 012001, (2018).

[11]. K. Deva Arun Kumar , S. Valanarasu , A. Kathalingam , V. Ganesh , Mohd. Shkir , and S. AlFaify , "Effect of solvents on sol-gel spin-coated nanostructured Al-doped ZnO thin films: a film for key optoelectronic applications", Applied Physics A 123:801, (2017).

[12]. K. S. Usha, R. Sivakumar and C. Sanjeeviraja, "Optical constant and dispersion energy of NiO thin films prepared by radio frequency magneto sputtering technique", J. Appl. Phys. 114, (2013), 123501-123510.

[13]. L. Kazmarski, and A Clark, "Polycrystalline and amorphous thin films and device", Edited by Lawrence Academic Press, New York , 267: 142 (1980).

[14]. M. A. Omar, "Elementary Solid State Physics", Addison-Wesley Publishing Company, Boston, (1993).

[15]. M. Caglar, S. Ilican and Y. Caglar, "Influence of substrate temperature on structural and electrical properties of ZnO films", Trakya Univ. J Sci, 7, No. 2, (2006) , 153-158.

[16]. M. Kanagaraj, P. Sathishkumar, G. Kalai Selvan, I. Phebe Kokila and S. Arumugam, "Structural and magnetic properties of $CuFe_2O_4$ as-prepared and thermally treated spinel nanoferrites", Indian Journal of Pure and Applied Physics, 52, (2014), 124-130.

[17]. M. Selim Soliman, G. Turky, M.A. Shouman and G.A. El-Shobaky, "Effect of Li_2O doping on electrical properties of $CoFe_2O_4$", Solid State Ionics, 120, (1999), 173-181.

[18]. M.I. Khan, K.A. Bhatti and Rabia Qindeel," Characterizations of multilayer ZnO thin films deposited by sol-gel spincoating technique", Journal of results in physics, No.7, (2017), 651- 655.

[19].Muhammad Tahir Farid , Ishtiaq Ahmad, and Muddassra Kanwal, "Effect of praseodymium ions on manganese based spinel ferrites", Chinese Journal of Physics 55, (2017) , 813-824.

[20]. Nguyen Kim Thanh, To Thanh Loan, Luong Ngoc Anh, Nguyen Phuc Duong, Siriwat Soontaranon, Nirawat Thammajak, and Than Duc Hien, "Cation distribution in $CuFe_2O_4$ nanoparticles: Effects of Ni doping on magnetic properties", Journal of Applied Physics 120, (2016), 142115.

[21]. P. J. Brown and j. B. Forsyth, "The crystal structure of solid", Arnold, (1973).

[22]. S. Majumder, "Synthesis and characterization of SnO_2 films obtained by a wet chemical process", Materials Science-Poland, 27, No. 1, (2009) , 123-129.

[23]. S. Rus, P. Vlazan, S. Novaconi, P. Sfirloaga and I. Grozescu, "Synthesis and characterization $CuFe_2O_4$ nanoparticles prepared by the hydrothermal ultrasonic assisted method",J. Optoelectron. Adv. Mater. 14, 293, (2012).

[24]. S. S. Kumbhar, M. A. Mahadik, V. S. Mohite, K. Y. Rajpure and C. H. Bhosale, "Synthesis and characterization of spray deposited nickel-zinc ferrite thin films", 4th International Conference on Advances in Energy Research, 54, (2014) , 599-605.

[25]. Satyendra Singh Chauhan, Chaturbhuj Ojha and A.K. Shrivastava, "Synthesis and characterization of $CuFe_2O_4$ nanoparticles" , International Journal of Theoretical and Applied Sciences, 1(2), (2009), 9-11.